Draft version February 12, 2025
Typeset using LaTeX **twocolumn** style in AASTeX631

On the prevalence of early mass transfer for very massive binaries

C. A. Burt,[1] M. Renzo,[1] A. Grichener,[1] and N. Shah[1]

[1] *University of Arizona, Department of Astronomy & Steward Observatory, 933 N. Cherry Ave., Tucson, AZ 85721, USA*

ABSTRACT

Common phases of mass transfer in massive stellar binaries are case A (during the donor's main sequence) and case B (after the donor's main sequence but before helium core depletion). Most stars see their radii significantly grow after the main sequence, making case B more common. However, very massive stars may already undergo significant expansion during the main sequence increasing the probability of case A mass transfer. We find that using convective boundary mixing informed by the width of the main sequence in 30 Doradus, case A mass transfer dominates for donor masses $\gtrsim 75\,M_\odot$. This is not the case without convective boundary mixing or in the stellar models commonly used in rapid binary population synthesis. Therefore, case A mass transfer may be more dominant than commonly assumed, with potential impact on rates of all post mass transfer binaries, from Wolf-Rayet-O-type binaries, to X-ray binaries and gravitational wave progenitors.

1. MASS TRANSFER IN VERY MASSIVE BINARIES

Binaries ~~stars~~ with ~~a sufficiently small~~ orbital separation $a \lesssim 2500\,R_\odot$ undergo (at least one) mass transfer phases (Sana et al. 2012)~~in which the donor star transfers mass to the initially less massive accretor~~. For very massive donors ($\gtrsim 30\,M_\odot$), mass transfer most often occurs during the donor's hydrogen ~~core-burning phase~~(case A) or helium core-burning phase (case B), which together account for $\sim 99\%$ of the ~~donor's~~ lifetime. ~~(Kippenhahn & Weigert 1967).~~

For a flat in $\log_{10}(a)$ initial ~~separation~~ distribution (Öpik 1924), case B is expected to be more common ~~to occur more often than case A mass transfer~~, since most stars expand dramatically post-main sequence (e.g., van den Heuvel 1969). However, very massive stars may already undergo a drastic expansion ~~in radius~~ during their main sequence (e.g., Sanyal et al. 2015; Jiang et al. 2015). This may increase the rate of case A (de Mink et al. 2008), ~~affecting the evolution of the star and consequently~~ potentially affecting ~~altering stellar parameters that determine the rate of~~ Wolf-Rayet+O-type binaries (e.g., Nuijten & Nelemans 2024), and X-ray binaries and gravitational wave progenitors (e.g., Mandel & Broekgaarden 2022).

The radius of the donor depends ~~is dependent~~ on poorly constrained stellar parameters, including ~~stellar~~ winds (Renzo et al. 2017; Josiek et al. 2024), metallicity (Xin et al. 2022), treatment of close-to-super-Eddington layers (e.g., Joss et al. 1973; Paxton et al. 2013; Jiang et al. 2015; Agrawal et al. 2022; Jermyn et al. 2023), rotation (e.g., Maeder & Meynet 2000) and consequently tides (e.g., Fabry et al. 2022) and convective boundary mixing (Anders & Pedersen 2023; Johnston et al. 2024). Here, we explore the radial evolution of very massive stars and its impact on when mass transfer starts. ~~We also show variations in convective boundary mixing and~~ and compare ~~them~~ to ~~stellar~~ models commonly adopted in rapid binary population synthesis.

2. COMPARING DONOR RADII

We computed MESA models[1] (version 24.03.1, Paxton et al. 2011, 2013, 2015, 2018, 2019; Jermyn et al. 2023) from $30\,M_\odot$ to $100\,M_\odot$ in steps of $5\,M_\odot$ at metallicity $Z = 0.001$ and 0.0001 following the setup from Renzo et al. (2023). The gray lines in Fig. 1 show their radial evolution as a function of time.

When using overshooting (top), we adopt ~~our MESA models implement~~ an exponential algorithm (Herwig 2000) fit to the step overshoot-

Corresponding author: C. A. Burt
caburt@arizona.edu

Corresponding author: M. Renzo
mrenzo@arizona.edu

[1] ~~Publicly~~ Available at doi.org/10.5281/zenodo.14757819

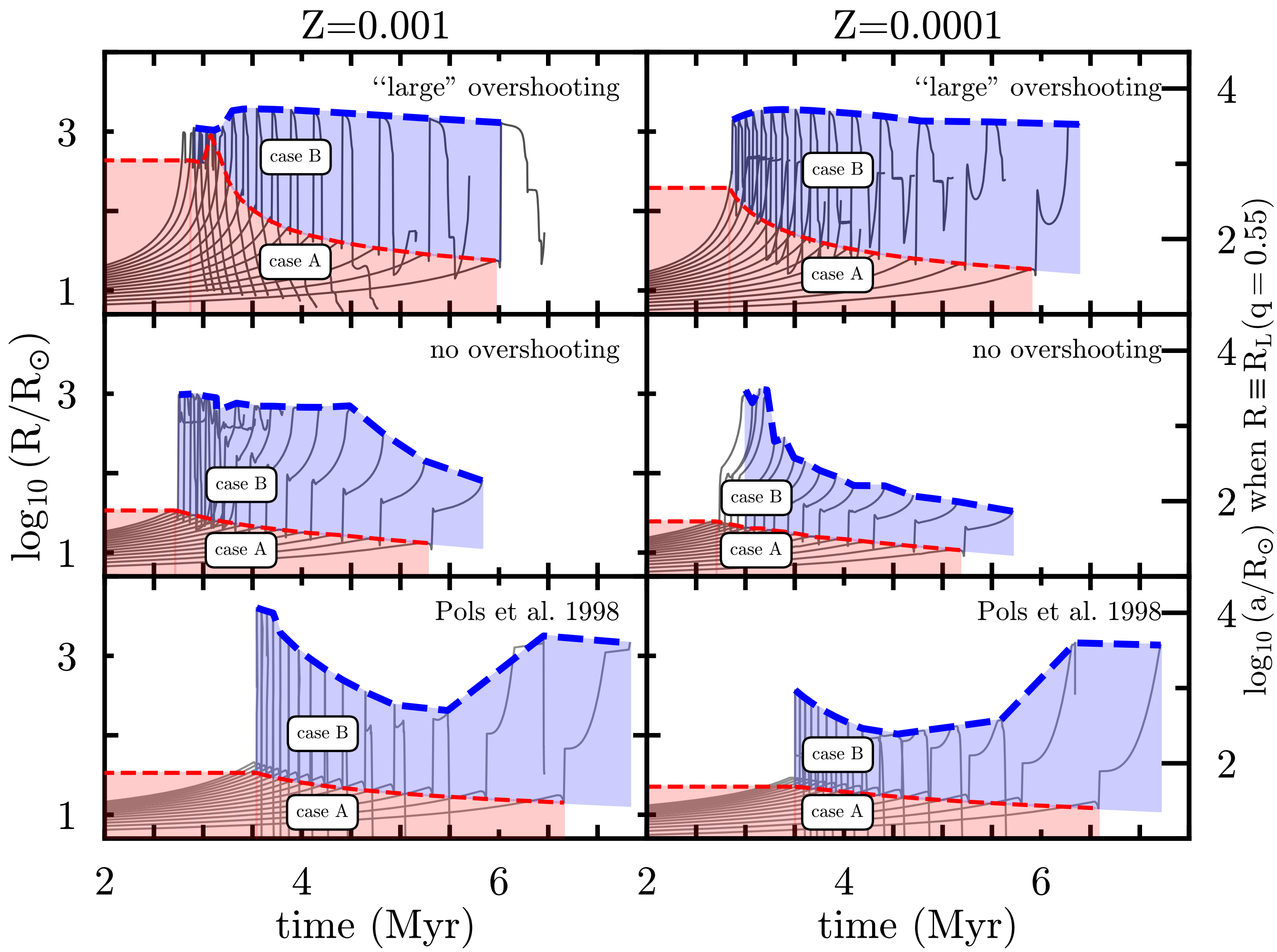

Figure 1. Each panel contains 15 stellar MESA models spanning from $30\,M_\odot$ star (longer lifetimes) to $100\,M_\odot$ (shorter lifetimes). The top panels show models with Brott et al. (2011)-like convective boundary mixing ("large" overshooting) (Claret & Torres 2018), the middle show models without overshooting, and the bottom panels plot models generated from COMPAS based on analytic fits to the stellar models of Pols et al. (1998). The left (right) panels have a metallicity $Z = 0.001$ ($Z = 0.0001$). Dashed red (blue) lines mark the maximum radius during the main sequence (during the runtime of the model). The red (blue) shaded areas underneath correspond to case A (case B) mass transfer.

ing calibrated on the width of main sequence in 30 Doradus ($\sim$ 0.335 pressure scale heights, Brott et al. 2011) following Claret & Torres (2018), corresponding to `(f,f_0)=(0.0415,0.008)`. We ~~compare this relatively "large overshooting" model with models including~~ we also compute models without any convective boundary mixing (middle), and show ~~to~~ the Pols et al. (1998) models including an effectively mass-dependent overshooting (bottom). These are the stellar models underpinning SSE (Hurley et al. 2000), which we generated using COMPAS (Stevenson et al. 2017; Vigna-Gómez et al. 2018; Riley et al. 2022). Models ~~We note that stars~~ with $M \geq 50\,M_\odot$ in the bottom panel are extrapolations. ~~SSE/COMPAS are the result of extrapolation of the fits to the models of Pols et al. (1998).~~

The red and blue dashed lines in each panel of Fig. 1 denote the maximum main sequence radius ~~during the main sequence (of the sampled masses)~~ and the maximum radius before helium depletion~~overall~~, marking the maximum Roche radius for a case A and case B donor, respectively. The right axis shows ~~orbital separations~~ a for which the star fills its Roche lobe~~where the stellar radius meets the roche radius computed from~~ Eggleton (1983), assuming a representative accretor-to-donor mass ratio ~~of~~ $q = 0.55$. ~~This value corresponds to the average for a flat mass-ratio distribu~~ ~~The red regions denote binaries which will undergo case A mass tr~~ For $Z = 0.001$, when including overshooting (top left panel), donors with masses $\gtrsim 75\,M_\odot$ ~~increasingly experience~~ are more likely to experience case A. Removing convective boundary mixing reduces the ~~increase in~~ stellar radii during the main sequence, preserving a window for case B. ~~the blue region above the red line for case B mass transfer at all sampled masses.~~ The overshooting implementation from Pols et al. (1998), while nonzero, still leaves a large window for case B up to at least 100 $M_{\odot}$. At an even lower metallicity of $Z = 0.0001$ (right), stars are more compact, and all models allow for case B mass transfer at all masses.

3. IMPLICATIONS FOR POST-MASS-TRANSFER BINARIES

~~Convective boundary mixing (Brott et al. 2011; Johnston et al. 2024) and metallicity (e.g., Xin et al. 2022) have a strong effec~~ After a thermal-timescale initial phase, Case A mass transfer occurs overall on a longer (nuclear) timescale, while case B occurs entirely on a much shorter (thermal) timescale (but see Klencki et al. 2022). Moreover, the dynamical stability of ~~the orbit during~~ mass transfer is sensitive to the evolutionary phase ~~of the stars involved~~ (e.g., Claeys et al. 2014). Therefore, whether a ~~given~~ binary experiences dynamically unstable interactions depends on ~~the size of~~ stellar radii ~~at the onset of mass transfer~~ and their reaction to mass changes, both in turn influenced by ~~poorly-constrained~~ stellar physics assumptions. ~~Comparing rows in Fig. 1 shows that the stellar evolution models c~~ Given the critical role of mass transfer ~~for the formation of many binaries of interest~~, the fraction of systems experiencing case A in respect to case B ~~may~~ significantly impacts predicted rates for post mass transfer binaries. ~~, including Wolf-Rayet+O-type binaries, X-ray binaries, and gravit~~ In particular, the role of the stable mass transfer channel (e.g., Marchant et al. 2021; van Son et al. 2022) for (massive) binary black hole mergers is an active topic of discussion. Our results highlight that stellar uncertainties influence the mode of mass transfer and consequently the outcomes.

Software: This work made use of the following software packages: `matplotlib` (Hunter 2007) and `python` (Van Rossum & Drake 2009), http://github.com/TeamCOMPAS/COMPAS, and https://docs.mesastar.org MESA. Software citation information aggregated using `The Software Citation Station` (Wagg & Broekgaarden 2024; Wagg et al. 2024).

REFERENCES

Agrawal, P., Stevenson, S., Szécsi, D., & Hurley, J. 2022, A&A, 668, A90, doi: 10.1051/0004-6361/202244044

Anders, E. H., & Pedersen, M. G. 2023, Galaxies, 11, 56, doi: 10.3390/galaxies11020056

Brott, I., de Mink, S. E., Cantiello, M., et al. 2011, A&A, 530, A115, doi: 10.1051/0004-6361/201016113

Cheng, S. J., Goldberg, J. A., Cantiello, M., et al. 2024, ApJ, 974, 270, doi: 10.3847/1538-4357/ad701e

Claeys, J. S. W., Pols, O. R., Izzard, R. G., Vink, J., & Verbunt, F. W. M. 2014, A&A, 563, A83, doi: 10.1051/0004-6361/201322714

Claret, A., & Torres, G. 2018, ApJ, 859, 100, doi: 10.3847/1538-4357/aabd35

de Mink, S. E., Pols, O. R., & Yoon, S. C. 2008, in American Institute of Physics Conference Series, Vol. 990, First Stars III, ed. B. W. O'Shea & A. Heger (AIP), 230–232, doi: 10.1063/1.2905549

Eggleton, P. P. 1983, ApJ, 268, 368, doi: 10.1086/160960

Fabry, M., Marchant, P., & Sana, H. 2022, A&A, 661, A123, doi: 10.1051/0004-6361/202243094

Herwig, F. 2000, A&A, 360, 952, doi: 10.48550/arXiv.astro-ph/0007139

Hunter, J. D. 2007, Computing in Science & Engineering, 9, 90, doi: 10.1109/MCSE.2007.55

Hurley, J. R., Pols, O. R., & Tout, C. A. 2000, MNRAS, 315, 543, doi: 10.1046/j.1365-8711.2000.03426.x

Jermyn, A. S., Bauer, E. B., Schwab, J., et al. 2023, ApJS, 265, 15, doi: 10.3847/1538-4365/acae8d

Jiang, Y.-F., Cantiello, M., Bildsten, L., Quataert, E., & Blaes, O. 2015, ApJ, 813, 74, doi: 10.1088/0004-637X/813/1/74

Johnston, C., Michielsen, M., Anders, E. H., et al. 2024, ApJ, 964, 170, doi: 10.3847/1538-4357/ad2343

Josiek, J., Ekström, S., & Sander, A. A. C. 2024, A&A, 688, A71, doi: 10.1051/0004-6361/202449281

Joss, P. C., Salpeter, E. E., & Ostriker, J. P. 1973, ApJ, 181, 429, doi: 10.1086/152060

Kippenhahn, R., & Weigert, A. 1967, ZA, 65, 251

Klencki, J., Istrate, A., Nelemans, G., & Pols, O. 2022, A&A, 662, A56, doi: 10.1051/0004-6361/202142701

Kobulnicky, H. A., & Fryer, C. L. 2007, ApJ, 670, 747, doi: 10.1086/522073

Maeder, A., & Meynet, G. 2000, ARA&A, 38, 143, doi: 10.1146/annurev.astro.38.1.143

Mandel, I., & Broekgaarden, F. S. 2022, Living Reviews in Relativity, 25, 1, doi: 10.1007/s41114-021-00034-3

Marchant, P., Pappas, K. M. W., Gallegos-Garcia, M., et al. 2021, A&A, 650, A107, doi: 10.1051/0004-6361/202039992

Nuijten, M., & Nelemans, G. 2024, arXiv e-prints, arXiv:2412.00938, doi: 10.48550/arXiv.2412.00938

Öpik, E. 1924, Publications of the Tartu Astrofizica Observatory, 25, 1

Paxton, B., Bildsten, L., Dotter, A., et al. 2011, ApJS, 192, 3, doi: 10.1088/0067-0049/192/1/3

Paxton, B., Cantiello, M., Arras, P., et al. 2013, ApJS, 208, 4, doi: 10.1088/0067-0049/208/1/4

Paxton, B., Marchant, P., Schwab, J., et al. 2015, ApJS, 220, 15, doi: 10.1088/0067-0049/220/1/15

Paxton, B., Schwab, J., Bauer, E. B., et al. 2018, ApJS, 234, 34, doi: 10.3847/1538-4365/aaa5a8

Paxton, B., Smolec, R., Schwab, J., et al. 2019, ApJS, 243, 10, doi: 10.3847/1538-4365/ab2241

Pols, O. R., Schröder, K.-P., Hurley, J. R., Tout, C. A., & Eggleton, P. P. 1998, MNRAS, 298, 525, doi: 10.1046/j.1365-8711.1998.01658.x

Renzo, M., Ott, C. D., Shore, S. N., & de Mink, S. E. 2017, A&A, 603, A118, doi: 10.1051/0004-6361/201730698

Renzo, M., Zapartas, E., Justham, S., et al. 2023, ApJL, 942, L32, doi: 10.3847/2041-8213/aca4d3

Riley, J., Agrawal, P., Barrett, J. W., et al. 2022, ApJS, 258, 34, doi: 10.3847/1538-4365/ac416c

Sana, H., de Mink, S. E., de Koter, A., et al. 2012, Science, 337, 444, doi: 10.1126/science.1223344

Sanyal, D., Grassitelli, L., Langer, N., & Bestenlehner, J. M. 2015, A&A, 580, A20, doi: 10.1051/0004-6361/201525945

Smith, N. 2014, ARA&A, 52, 487, doi: 10.1146/annurev-astro-081913-040025

Stevenson, S., Vigna-Gómez, A., Mandel, I., et al. 2017, Nature Communications, 8, 14906, doi: 10.1038/ncomms14906

van den Heuvel, E. P. J. 1969, AJ, 74, 1095, doi: 10.1086/110909

Van Rossum, G., & Drake, F. L. 2009, Python 3 Reference Manual (Scotts Valley, CA: CreateSpace)

van Son, L. A. C., de Mink, S. E., Renzo, M., et al. 2022, ApJ, 940, 184, doi: 10.3847/1538-4357/ac9b0a

Vigna-Gómez, A., Neijssel, C. J., Stevenson, S., et al. 2018, MNRAS, 481, 4009, doi: 10.1093/mnras/sty2463

Wagg, T., Broekgaarden, F., & Gültekin, K. 2024, TomWagg/software-citation-station: v1.2, v1.2, Zenodo, doi: 10.5281/zenodo.13225824

Wagg, T., & Broekgaarden, F. S. 2024, arXiv e-prints, arXiv:2406.04405. https://arxiv.org/abs/2406.04405

Xin, C., Renzo, M., & Metzger, B. D. 2022, MNRAS, 516, 5816, doi: 10.1093/mnras/stac2551